Plant Communications
Correspondence

CellPress
Partner Journal

Genome-edited ATP BINDING CASSETTE B1 transporter SD8 knockouts show optimized rice architecture without yield penalty

Dear editor,

In the 1960s, the use of semi-dwarf rice and wheat varieties ushered in the "Green Revolution," leading to reduced lodging and increased harvest index. In rice, essentially all modern semi-dwarf varieties carry a specific null mutation or weak alleles of *Semi-Dwarf1 (SD1)*, which encodes a GA20-2 oxidase in the gibberellin biosynthetic pathway (Monna et al., 2002; Sasaki et al., 2002; Spielmeyer et al., 2002). In addition to gibberellins, other plant hormones such as brassinosteroids, strigolactones, and auxin also function in reducing rice height (Ferrero-Serrano et al., 2019). However, many dwarf or semi-dwarf mutants have not been widely used in rice-breeding programs because they adversely impact grain yield (Ferrero-Serrano et al., 2019). Moreover, the flag leaf has a higher photosynthetic capacity than lower canopy leaves, which allows for greater interception of light. Rice yield is closely related to the flag leaf because it contributes about 50% of the assimilates used to fill the grain with starch (Dong et al., 2018). Crops with erect flag leaves can grow at higher plant densities without compensatory reductions in photosynthesis, leading to increased grain yield. Therefore, dwarfing and leaf erectness have been breeding targets for several decades, as components of ideal plant architecture. Identification of genes that moderately reduce rice height (semi-dwarfing) and optimize rice architecture without yield penalty is still highly desirable.

Using data from a previous genome-wide association study, we analyzed single-nucleotide polymorphisms (SNPs) associated with rice height in the 3000 rice genomes dataset (Alexandrov et al., 2015; Wang et al., 2018) and successfully identified one predicted open reading frame, *Semi-Dwarf in chr8* (*SD8*, *LOC_Os08g45030*), in a 50-kb interval (28,270,000–28,280,000) of chromosome 8 (Figure 1A). Through phylogenetic analysis, we found that *SD8* encodes a putative ortholog of *Arabidopsis thaliana* ATP Binding Cassette B1 (ABCB1)/P-glycoprotein1 (Noh et al., 2003; Geisler et al., 2005). To investigate the biological functions of *SD8* in rice, we used CRISPR-Cas9-mediated gene editing to obtain two knockout (KO) lines in the Nipponbare (NIP) background (Figure 1B). Phenotypically, *sd8-1* (one-bp insertion mutant) and *sd8-2* (two-bp deletion mutant) plants had moderately reduced height due to shorter internode lengths, as well as a smaller flag-leaf angle, and thus displayed optimized plant architecture (Figures 1B–1D; supplemental Figure 1). *sd8* mutant phenotypes could be rescued in transgenic complementation lines (supplemental Figure 2). Notably, there were no significant phenotypic differences between NIP and the two *sd8* mutants in seven yield-related traits (supplemental Figures 2E–2I and 3). Because of the desirable possibility that the combination of semi-dwarf height and leaf angle in *sd8* could increase production yields under dense planting, we investigated yields of NIP and *sd8-1* in paddy-field plots at two planting densities. In the high-density plots (560,000 plants/ha), *sd8-1* mutants and NIP plants showed yield increases of ~20.6% and ~10%, respectively, compared with those grown in low-density plots. There was no significant difference in yield between genotypes grown in the low-density plots (280,000 plants/ha) (Figures 1E and 1F; supplemental Figure 4). Collectively, these data revealed that loss of *SD8* function could optimize rice architecture by reducing plant height and flag-leaf angle without yield penalty and that *SD8* KOs may even have the potential for increased yield under high-density planting.

Consistent with *sd8* mutant phenotypes, β-glucuronidase reporter assays and quantitative real-time PCR indicated that *SD8* was primarily expressed in the internode (Figure 1G; supplemental Figure 5A). *SD8* also showed differences in expression among seven *japonica* and *indica* cultivars (supplemental Figure 5B). We observed that SD8 was localized in the plasma membrane (supplemental Figure 5C). In plants, ABCB1 homologs are known to mediate cellular efflux of indole-3-acetic acid (IAA) and to regulate polar auxin transport (Multani et al., 2003; Noh et al., 2003; Geisler et al., 2005). We therefore measured the endogenous IAA content in NIP, *sd8-1*, and *sd8-2* seedlings. IAA levels were significantly lower in *sd8* than in NIP seedlings (Figure 1H). Moreover, we found that the shortened plant height and reduced leaf-angle phenotypes of *sd8* mutants could be rescued by applying exogenous IAA (supplemental Figure 6). Consistent with the observed reduction in auxin concentration, *sd8* mutants had reduced expression of genes in the auxin signaling pathway, including *OsPIN1a/1b/2* and *OsIAA3/9/20* (Figure 1I).

To further investigate whether *SD8* modulated auxin transport in rice, we measured IAA flux speed in NIP and *sd8-1* seedlings. IAA efflux and influx currents were significantly lower in *sd8-1* than in NIP, both with and without IAA treatment (Figure 1J), suggesting that loss of *SD8* function affected IAA flux currents. In addition, we used a previously reported assay to measure auxin acquisition in the IAA-sensitive yeast strain *yap1-1* (Yang et al., 2020) and found that SD8 indeed promoted IAA accumulation in yeast, resulting in a stronger suppression of IAA-induced growth (Figure 1K).

To determine whether *SD8* had similar biological functions and loss-of-function mutant phenotypes in diverse rice varieties, we

Published by the Plant Communications Shanghai Editorial Office in association with Cell Press, an imprint of Elsevier Inc., on behalf of CSPB and CEMPS, CAS.

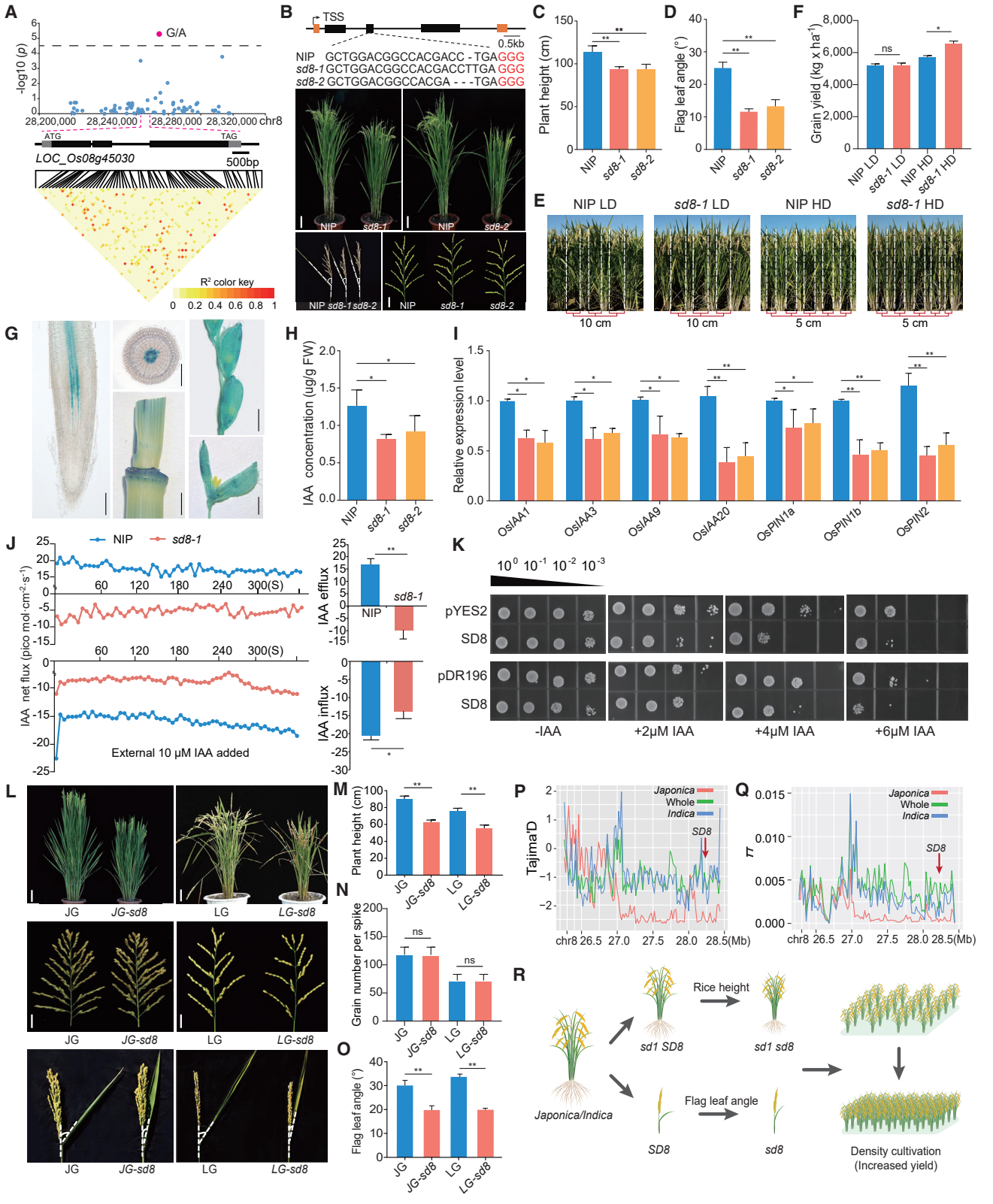

Figure 1. *SD8* knockouts showed reduced plant height and flag-leaf angle without yield penalty.

(**A**) Identification of a putative open reading frame on chromosome 8 (*LOC_08g45030*) associated with plant height based on re-analysis of SNPs in the 3000 rice genomes dataset (Alexandrov et al., 2015).

(legend continued on next page)

created CRISPR-Cas9-edited *SD8* KO mutants in two key elite cultivars in the *japonica* background, Jingeng818 (JG) and Longgeng31 (LG). Similar to the *SD8* KO plants in the NIP background, we observed a remarkable decrease in height and flag-leaf angle in *JG-sd8* and *LG-sd8* but no differences in the examined yield-related traits (Figures 1L–1O; supplemental Figure 7). We detected a considerable decrease in IAA content in these KO lines, and auxin-responsive gene expression was reduced in *JG-sd8* and *LG-sd8* (supplemental Figure 8). We also knocked out *SD8* in the *indica* rice cultivars 93-11, YexiangB (YX), Nongxiang32, and Yuzhenxiang. Similar to the *SD8* KO plants in the *japonica* background (NIP, JG, and LG), the KO lines in *indica* backgrounds also exhibited semi-dwarf phenotypes (Figure S9) and significant decreases in IAA content (Figure S10). Together, these results showed that loss of *SD8* function in different backgrounds could indeed reduce rice height and flag-leaf angle, suggesting an essential role for *SD8* in the optimization of rice architecture.

Analyses of SNPs and haplotypes (Haps) have become a major strategy for understanding evolutionary relationships and phenotypic variations, and these methods have breeding applications in rice (Wang et al., 2018). In the 3000 rice genomes dataset (Alexandrov et al., 2015), we identified 14 Haps using 16 SNPs in *SD8* (supplemental Figure 11A). The Hap frequencies differed significantly between the *indica* and *japonica* subspecies (supplemental Figures 11B and 11C). Next, we revealed significant differences in rice height among the top five most frequent Haps; Hap4 showed a significantly lower mean height than the other four Haps (supplemental Figure 11D). Based on Hap frequencies in *SD8*, we found that the *japonica* population had significantly higher Tajima's D and π (nucleotide diversity) values than the *indica* population in the ~2-Mb region flanking *SD8* (Figures 1P and 1Q). These data indicated that *SD8* has undergone strong balancing selection in the *japonica* subpopulation, suggesting that there is considerable potential for using *SD8* to balance increased productivity and reduced height.

The discovery of the semi-dwarfism gene *SD1* enabled the introduction of dwarfism to breeding programs in the 1960s, a major scientific advance for the rice Green Revolution. *SD1* has undergone significant artificial selection in *japonica* and *indica rice* cultivars (Asano et al., 2011), and different mutant alleles of *SD1* have been used separately for rice breeding in the *japonica* or *indica* background to produce semi-dwarf cultivars. The *indica* cultivars contain loss-of-function *SD1* mutations, and the *japonica* cultivars contain weak alleles. Based on previous reports, *japonica* cultivars NIP and LG contain weak *sd1* mutant alleles (*sd1-EQ type*), and *indica* cultivars YX and 9311 are considered to contain loss-of-function mutant alleles (s*d1-d* allele type for YX, and dwarf *sd1-9311* type for 9311) (Asano et al., 2011; Wu et al., 2018). Despite the many advantages of *sd1* as a source of dwarfism and lodging resistance, its widespread use has been revealed to have other associated negative effects. It has been reported that mutation of *SD1* has negative effects on spikelet number per panicle, panicle length, and branch number, eventually resulting in reduced yield (Murai et al., 2002; Su et al., 2021). Like mutation of *SD1* in modern *indica* and *japonica* cultivars, we propose that genome editing of *SD8* may have similar potential for reducing the height of *indica* and *japonica rice* cultivars (Figure 1Q). In addition, *sd8* mutation could also reduce flag-leaf angle without yield penalty. Thus, we believe that *SD8* could be an alternative dwarfing gene for rice-breeding programs and that it has more potential to further reduce rice height or even increase yield under high-density planting. The application of sophisticated genome-editing technology to *SD8* enabled us to develop sustainable rice varieties with optimized architecture and without yield penalty. This approach has the potential to revolutionize direct-seeding strategies for green-agriculture cultivation of rice.

The *Arabidopsis abcb1* mutant does not show a dwarf phenotype, in contrast to the semi-dwarf and reduced flag-leaf-angle phenotypes of *sd8* in rice (Noh et al., 2003; Geisler et al., 2005). Although mutation of ABCB1 homologs in the monocots maize (*br2*) and sorghum (*dw3*) causes a severe dwarf phenotype, grain yield is also severely reduced (Multani et al., 2003), which may hinder the application of ABCB1 homologs to the breeding of semi-dwarf plants. It will be crucial to determine whether ABCB1 homologs have conserved functional effects on auxin transport but different KO phenotypes in various plant lineages.

(**B**) Gross phenotypes of *SD8* KO lines in the Nipponbare (NIP) background obtained using CRISPR-Cas9 gene editing. Top panel: mutation sites in the two knockout lines (*sd8-1* and *sd8-2*). Bottom panels: height, flag-leaf angle, and panicle morphology in NIP, *sd8-1*, and *sd8-2* plants.
(**C** and **D**) Comparison of plant height (**C**) and flag-leaf angle (**D**) between NIP, *sd8-1*, and *sd8-2* plants.
(**E**) Representative NIP and *sd8-1* plants grown under different planting densities. Seeds from NIP and *sd8-1* were grown at high (5 × 20 cm) and low (10 × 20 cm) planting densities.
(**F**) Grain yield of NIP and *sd8-1* plants grown at high and low planting densities. ns, not significant. *$p < 0.01$ (Student's *t*-test).
(**G**) Glucuronidase staining in roots of 7-day-old seedlings, internodes at the early heading stage, glumes at the early heading stage, and glumes at the late heading stage. Scale bars: 1 mm.
(**H**) Gas chromatography–mass spectroscopy analysis of endogenous free IAA concentrations in NIP, *sd8-1*, and *sd8-2* seedlings.
(**I**) Relative expression levels of *OsIAA1/3/9/20* and *OsPIN1a/1b/2* in aerial tissues of 3-week-old NIP, *sd8-1*, and *sd8-2* seedlings.
(**J**) Time course analysis of IAA efflux and net influx in the primary root meristem of 7-day-old NIP and *sd8-1* seedlings as measured continuously for 5 min by the scanning ion-selective electrode technique. IAA influx was measured in the presence of 10 μM exogenous IAA. Columns represent the mean net influx rates averaged over the entire 5-min observation window (±SE, n = 6–10 plants). *$p < 0.05$ (one-way analysis of variance).
(**K**) *SD8* functionality assays for auxin acquisition in the IAA-sensitive yeast strain *yap1-1*. The growth status is shown for *yap1-1* cells expressing empty vectors (pYES2 and pDR196) and *SD8* on SD-U medium without uracil supplemented with 2, 3, 4, or 6 μM IAA. Serial dilutions (1:10) of yeast cells were spotted onto SD-U solid medium containing 2% galactose or glucose, then incubated at 30°C for 4 to 6 days.
(**L**) Gross phenotypes of *SD8* KO lines in the Jingeng818 and Longgeng31 backgrounds.
(**M**–**O**) Quantitative analysis of plant height and flag-leaf angle in wild-type and *SD8* KO lines in the Jingeng818 and Longgeng31 backgrounds.
(**P** and **Q**) Tajima's D and nucleotide diversity (π) values for a ~2-Mb genomic region flanking *SD8* in the 3000 rice genomes dataset.
(**R**) A model for loss of *SD8* function with and without *SD1* in which plant height is reduced but yield is increased under high-density planting.

SUPPLEMENTAL INFORMATION

Supplemental information is available at *Plant Communications Online*.

FUNDING

This work was supported by grants from the National Natural Science Foundation of China (32130080) to X.G., the Central Public-interest Scientific Institution Basal Research Fund (Y2022PT22) to X.G., the Agricultural Science and Technology Innovation Program (CAAS-ZDRW202109), the Hainan Yazhou Bay Seed Laboratory (B21HJ0223) to X.G., and the Key Technologies R & D Program of Tianjin (18YFZCNC01210) to S.Y.

AUTHOR CONTRIBUTIONS

X.G., S.Y., and L.Y. supervised the project. R.Q., P.Z., and Q.L. performed most of the experiments. Y.W. and W.G. analyzed the data. Z.D. and X.L. assisted with the experiments. P.Z. and X.G. wrote the manuscript. P.Z., R.Q., and X.G. revised the manuscript. All authors read and approved the final manuscript.

ACKNOWLEDGMENTS

No conflict of interest is declared.

Received: May 7, 2022
Revised: May 29, 2022
Accepted: June 6, 2022
Published: June 10, 2022

Ruihong Qu[1,5], Pingxian Zhang[2,5], Qing Liu[4,5], Yifan Wang[1], Weijun Guo[1], Zhuoying Du[1], Xiulan Li[1], Liwen Yang[1,], Shuangyong Yan[3,*] and Xiaofeng Gu[1,*]*

[1]Biotechnology Research Institute, Chinese Academy of Agricultural Science, Beijing 100081, China
[2]College of Life Science and Technology, Huazhong Agricultural University, Wuhan, 430070 Hubei, China
[3]Tianjin Key Laboratory of Crop Genetics and Breeding, Tianjin Crop Research Institute, Tianjin Academy of Agricultural Sciences, Tianjin 300384, China
[4]College of Life Sciences, Hebei Agricultural University, Baoding, 071001 Hebei, China
[5]These authors contributed equally
***Correspondence: Liwen Yang (yangliwen@caas.cn), Shuangyong Yan (bioysy@139.com), Xiaofeng Gu (guxiaofeng@caas.cn)**

https://doi.org/10.1016/j.xplc.2022.100347

REFERENCES

Alexandrov, N., Tai, S., Wang, W., Mansueto, L., Palis, K., Fuentes, R.R., Ulat, V.J., Chebotarov, D., Zhang, G., Li, Z., et al. (2015). SNP-Seek database of SNPs derived from 3000 rice genomes. Nucleic Acids Res. **43**:D1023–D1027. https://doi.org/10.1093/nar/gku1039.

Asano, K., Yamasaki, M., Takuno, S., Miura, K., Katagiri, S., Ito, T., Doi, K., Wu, J., Ebana, K., Matsumoto, T., et al. (2011). Artificial selection for a green revolution gene during *japonica* rice domestication. Proc. Natl. Acad. Sci. U S A. **108**:11034–11039. https://doi.org/10.1073/pnas.1019490108.

Dong, H.J., Zhao, H., Li, S.L., Han, Z.M., Hu, G., Liu, C., Yang, G.Y., Wang, G.W., Xie, W.B., and Xing, Y.Z. (2018). Genome-wide association studies reveal that members of bHLH subfamily 16 share a conserved function in regulating flag leaf angle in rice (*Oryza sativa*). PLoS Genet. **14**:e1007323. https://doi.org/10.1371/journal.pgen.1007323.

Ferrero-Serrano, Á., Cantos, C., and Assmann, S.M. (2019). The role of dwarfing traits in historical and modern agriculture with a focus on rice. Cold Spring Harb. Perspect. Biol. **11**:a034645. https://doi.org/10.1101/cshperspect.a034645.

Geisler, M., Blakeslee, J.J., Bouchard, R., Lee, O.R., Vincenzetti, V., Bandyopadhyay, A., Titapiwatanakun, B., Peer, W.A., Bailly, A., Richards, E.L., et al. (2005). Cellular efflux of auxin catalyzed by the *Arabidopsis* MDR/PGP transporter AtPGP1. Plant J. **44**:179–194. https://doi.org/10.1111/j.1365-313x.2005.02519.x.

Multani, D.S., Briggs, S.P., Chamberlin, M.A., Blakeslee, J.J., Murphy, A.S., and Johal, G.S. (2003). Loss of an MDR transporter in compact stalks of maize *br2* and sorghum *dw3* mutants. Science **302**:81–84. https://doi.org/10.1126/science.1086072.

Monna, L., Kitazawa, N., Yoshino, R., Suzuki, J., Masuda, H., Maehara, Y., Tanji, M., Sato, M., Nasu, S., and Minobe, Y. (2002). Positional cloning of rice semidwarfing gene, *sd-1*: rice "green revolution gene" encodes a mutant enzyme involved in gibberellin synthesis. DNA Res. **9**:11–17. https://doi.org/10.1093/dnares/9.1.11.

Murai, M., Takamure, I., Sato, S., Tokutome, T., and Sato, Y. (2002). Effects of the dwarfing gene originating from 'Dee-geo-woo-gen' on yield and its related traits in rice. Breed Sci. **52**:95–100. https://doi.org/10.1270/jsbbs.52.95.

Noh, B., Bandyopadhyay, A., Peer, W.A., Spalding, E.P., and Murphy, A.S. (2003). Enhanced gravi- and phototropism in plant mdr mutants mislocalizing the auxin efflux protein PIN1. Nature **423**:999–1002. https://doi.org/10.1038/nature01716.

Spielmeyer, W., Ellis, M.H., and Chandler, P.M. (2002). Semidwarf (*sd-1*), "green revolution" rice, contains a defective *gibberellin 20-oxidase gene*. Proc. Natl. Acad. Sci. U S A. **99**:9043–9048. https://doi.org/10.1073/pnas.132266399.

Sasaki, A., Ashikari, M., Ueguchi-Tanaka, M., Itoh, H., Nishimura, A., Swapan, D., Ishiyama, K., Saito, T., Kobayashi, M., Khush, G.S., et al. (2002). Green revolution: a mutant gibberellin-synthesis gene in rice. Nature **416**:701–702. https://doi.org/10.1038/416701a.

Su, S., Hong, J., Chen, X., Zhang, C., Chen, M., Luo, Z., Chang, S., Bai, S., Liang, W., Liu, Q., et al. (2021). Gibberellins orchestrate panicle architecture mediated by DELLA-KNOX signaling in rice. Plant Biotechnol. J. **19**:2304–2318. https://doi.org/10.1111/pbi.13661.

Wang, W., Mauleon, R., Hu, Z., Chebotarov, D., Tai, S., Wu, Z., Li, M., Zheng, T., Fuentes, R.R., Zhang, F., et al. (2018). Genomic variation in 3, 010 diverse accessions of Asian cultivated rice. Nature **557**:43–49. https://doi.org/10.1038/s41586-018-0063-9.

Wu, Z., Tang, D., Liu, K., Miao, C., Zhuo, X., Li, Y., Tan, X., Sun, M., Luo, Q., and Cheng, Z. (2018). Characterization of a new semi-dominant dwarf allele of *SLR1* and its potential application in hybrid rice breeding. J. Exp. Bot. **69**:4703–4713. https://doi.org/10.1093/jxb/ery243.

Yang, T., Feng, H., Zhang, S., Xiao, H., Hu, Q., Chen, G., Xuan, W., Moran, N., Murphy, A., Yu, L., et al. (2020). The potassium transporter OsHAK5 alters rice architecture via ATP-dependent transmembrane auxin fluxes. Plant Commun. **1**:100052. https://doi.org/10.1016/j.xplc.2020.100052.

Plant Communications, Volume *3*

Supplemental information

Genome-edited ATP BINDING CASSETTE B1 transporter SD8 knock-outs show optimized rice architecture without yield penalty

Ruihong Qu, Pingxian Zhang, Qing Liu, Yifan Wang, Weijun Guo, Zhuoying Du, Xiulan Li, Liwen Yang, Shuangyong Yan, and Xiaofeng Gu

SUPPLEMENTAL INFORMATION

Genome-edited ATP BINDING CASSETTE B1 transporter SD8 knockouts have optimized rice architecture without yield penalty

Ruihong Qu[1,5], Pingxian Zhang[2,5], Qing Liu[4,5], Yifan Wang[1], Weijun Guo[1], Zhuoying Du[1], Xiulan Li[1], Liwen Yang[1,*], Shuangyong Yan[3,*], Xiaofeng Gu[1,*]

[1]Biotechnology Research Institute, Chinese Academy of Agricultural Science, Beijing 100081, China

[2]College of Life Science and Technology, Huazhong Agricultural University, Wuhan 430070, Hubei, China

[3]Tianjin Key Laboratory of Crop Genetics and Breeding, Tianjin Crop Research Institute, Tianjin Academy of Agricultural Sciences, Tianjin 300384, China

[4]College of life sciences, Hebei agricultural university, Baoding 071001, Hebei, China

[5]These authors contributed equally.

***Correspondence:** Liwen Yang (yangliwen@caas.cn), Shuangyong Yan (bioysy@139.com), Xiaofeng Gu (guxiaofeng@caas.cn)

This PDF file includes:

SI Materials and Methods

Figures S1 to S11 and Tables S1

SI References

List of Supplemental Information:

SI Materials and Methods

Plant materials and growth conditions

In this study, seven cultivars of rice (*Oryza sativa* L.) were used for creating CRISPR/Cas9 gene-editing lines, namely, three *japonica* cultivars Nipponbare (NIP), Jinggeng818 (JG), and Longgeng31 (LG), and four *indica* cultivars 9311, YexiangB (YX), Nongxiang32 (NX), and Yuzhenxiang (YZX). For phenotypic analysis, the plants were spaced 30 cm apart and grown at the Chinese Academy of Agricultural Sciences in Beijing (39°54'N, 116°23'E), China, from May to October of each year. For hormone analysis, rice plants were planted in water-soaked sand for germination, and after 3 days seeds were transferred into normal culture solution. Rice plants were grown in growth chambers with 60–70% humidity and a light/dark cycle of 12/12 h at 30/24°C.

Transgene constructs and targeted gene editing

To generate knockout plants using CRISPR/Cas9 technology, single-guide RNA targeting 5′- GCTGGACGGCCACGACCTGA -3′ was cloned downstream of the *OsU6* promoter in the CRISPR/Cas9 binary vector BGK032 (Biogle Technology). These constructs were introduced into diverse rice backgrounds (two *japonica* varieties (Jingeng818 (JG) and Longgeng31 (LG)) and four *indica* varieties (Nongxiang32 (NX), 93-11, YexiangB (YX), and Yuzhenxiang (YZX)) by Agrobacterium-mediated transformation using standard protocols. For complementation of the *SD8-1* mutant, a DNA fragment containing the 2000 bp promoter and the full-length protein-coding sequence of *SD8*/*OsABCB1* (CDS: 4,035 bp) was amplified and inserted into a binary vector p23A between KpnI sites. For *SD8* overexpression, the full-length

SD8/*OsABCB1* protein-coding sequence was amplified from NIP and cloned into the vector pBS-2, then introduced into the plant binary vector pCAMBIA1304 to generate the fusion *pCaMV35S::SD8*. The transgenic rice plants were confirmed by quantitative real-time PCR (qPCR) or PCR detection and direct sequencing.

Subcellular localization

A vector containing *p35S::SD8-GFP* was transiently expressed in rice protoplasts as described previously (Geng et al., 2020; Zhang et al., 2021). GFP fluorescence signals were observed and recorded using a Zeiss LSM 700 confocal laser-scanning microscope.

***Pro: SD8-GUS* analysis**

The *proSD8::GUS* transgenic plants were grown in standard rice culture solution. GUS staining of tissues was carried out as described previously (Zhang et al., 2021).

qRT-PCR assays

Total RNA was prepared using RNeasy Plant Mini kit (Qiagen) and then contaminating genomic DNA was removed by digestion with recombinant DNase I (RNase-free, TAKARA) following the manufacturer's instructions. qRT-PCR was performed using SYBR Green Supermix (TOYOBO) on an Applied Biosystems 7500 Fast real-time PCR system. Relative expression of the selected genes was analyzed using the $2^{-\Delta\Delta CT}$ method (Zhang et al., 2021).

Quantification of IAA content and flux in rice plants

Endogenous free IAA in rice plant 3 weeks seedling were quantified by gas chromatography-mass spectrometry (GC-MS) as described in Henrichs et al. (2012).

The measurements were carried out using a GC-MS system at the Central Laboratory of Biotechnology Research Institute, Chinese Academy of Agricultural Sciences.

IAA fluxes were monitored non-invasively in the roots of plants grown for 7 days in hydroponic solutions using SIET (model BIO-003A; Younger USA Science and Technology, Falmouth, MA, USA, and Xu-Yue Science and Technology, Beijing, China; http://www.xuyue.net) containing an IAA-sensitive amperometric sensor based on a carbon nanotube-coated external oxidizing platinum microelectrode as described previously (Henrichs et al., 2012; Yang et al.,2020). The net influx current was defined as the difference between currents recorded in the absence and presence of exogenous 10 mM IAA. Fluxes were measured in the roots of at least 6-10 individual plants in two independent experiments.

SD8/OsABCB1 functionality assays for auxin acquisition in the IAA-sensitive yeast strain *yap1-1*

The whole open reading frames of *SD8* was amplified by PCR from cDNA of rice using forward primers SD8F (5'-CGGAATTCATGGAGGAGGAGATAAAGGG-3'), with an EcoRI site incorporated at the 5' end, and reverse primers SD8R (5'-CCG CTCGAGCTAGGTGCCGTGTGTTGTTGTTG-3'), with an XhoI site incorporated at the 3' end. After EcoRI and XhoI double enzyme digestion, the fragment was inserted between the EcoRI and XhoI sites of yeast expression vectors pYES2 and pDR196 (Yang et al., 2014). Subsequently, plasmids of pYES2, pDR196, *pYES2-SD8*, and *pDR196-SD8* were transformed into the IAA-sensitive mutant strain (S. cerevisiae) yap1-1 (Prusty et al., 2004) as described previously (Yang et al., 2014). Positive transformants were selected on glucose containing solid SD-U medium without uracil, and single colonies were grown in liquid SD-U medium supplemented with 2%

galactose or glucose. For functionality assays, transformants grown in liquid SD-U medium to an OD600 of approximately 0.6 were washed and diluted to OD600 in deionized water. Cells were diluted 10-fold three times, and 3 ml of each dilution was spotted onto an SD-U medium plate supplemented with the indicated concentrations of IAA. The plates were incubated at 30℃ for 3-5 days. The assays were performed with three independent transformants.

Yield-related trait measurements

All yield traits were measured when the plants had attained maturity. Panicle length, grain length, yield per plant, seed setting rate, and 1,000-grain weight were recorded. Yield per plant was scored as the total weight of grains from the entire plant. The number of tillers per plant was scored as the number of reproductive tillers for each plant. And 1,000-grain weight were measured using an automatic seed counting and analyzing instrument (Model SC-G; Wanshen). Plant height and panicle length were measured and analyzed.

GWAS analysis

The SNPs data on rice height (at the mature stage) were originated from previously reported 3k RG database (Wang et al., 2018). Briefly, we selected 3k RG 404k Core SNPs (MAF > 0.05 and missing rate <50%) to perform GWAS of plant height. The GWAS was conducted with a mixed linear model that was implemented in TASSEL v5.0 (Bradbury et al., 2007). We then selected $p=2.78\times10^{-5}$ (Benjamini–Hochberg FDR < 0.05) as the genome-wide significant cutoff followed by a previously conducted GWAS analysis (Duan et al., 2017).

Population genetic analysis of *SD8*

The haplotypes of *SD8* in the 3k RG were classified according to all SNPs with minor allele frequency>0.01 within the CDS region using the RFGB v2.0 database. The haplotypes in at least 100 rice accessions were used for comparative analysis of plant height traits, which were downloaded from the Rice SNP-Seek Database (Alexandrov N et al., 2015). One-way ANOVA followed by Duncan's new multiple-range test was performed with the agricolae package in *R*. Haplotype networks were constructed using the pegas package in *R*. Nucleotide diversity (π) and Tajima's D for each 50-kb window across the genome, with an overlapping 5-kb step size, were calculated for the 2-Mb region flanking *SD8* with the Variscan software (v2.0.3) (Vilella A et al.,2005).

Yield evaluation under different planting densities

Paddy trials were performed at the Chinese Academy of Agricultural Sciences in Beijing (39°54'N, 116°23'E), China, from May to October of each year. For NIP and *sd8-1* lines, each rice plant was grown in a paddy field at a distance of 20x10 cm (280,000 plants/ha), and 20x5 cm (560,000 plants/ha). Each treatment was performed in three individual plots with randomized blocks. A hundred rice plants were harvested and used for analysis from each plot excluding marginal plants. After harvest, the samples were dried for 14 days at 37℃ prior to measurements.

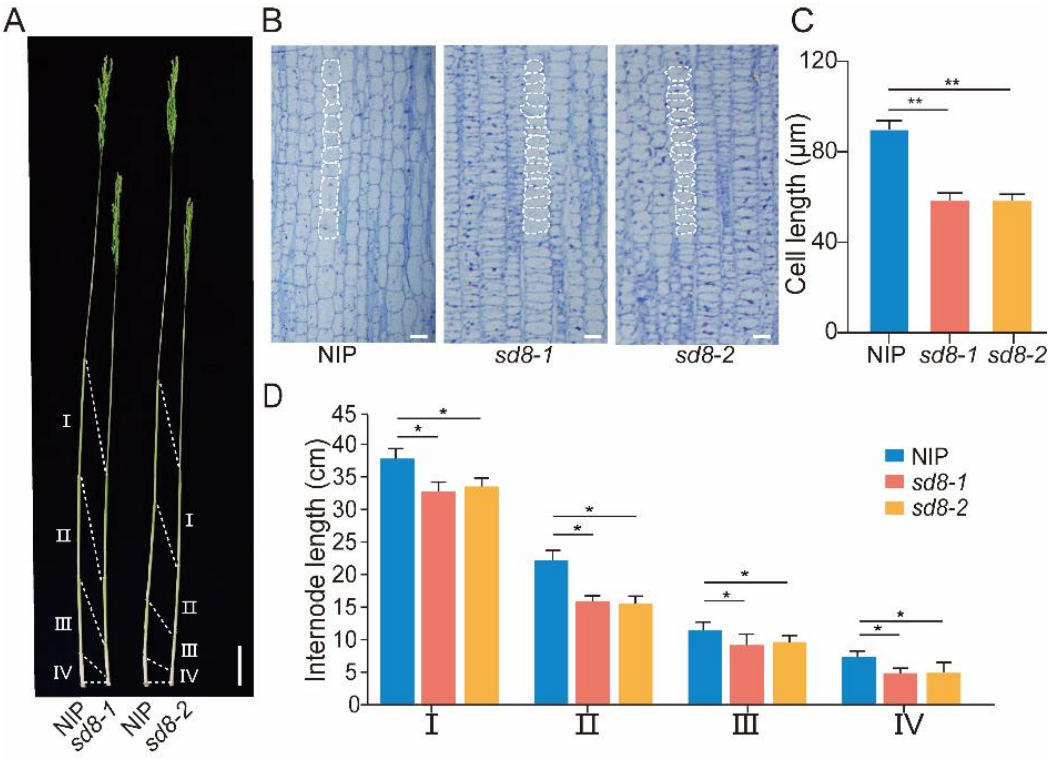

Supplementary Figure 1. *SD8* knockout (KO) lines reduced the length of the main culms.

(A) Main culms of wild-type (NIP) and *SD8* knockout lines (*sd8-1* and *sd8-2*). Arrows indicate nodes (scale bar:10 cm).

(B) Longitudinal sections of the elongated regions of the uppermost internodes of NIP, *sd8-1,* and *sd8-2* (Scale bars:50 μm for the longitudinal sections).

(C) Statistical data of the cell length in the longitudinal sections in B.

(D) Internode lengths of *SD8* KO lines (*sd8-1* and *sd8-2*) and NIP rice plants. Data indicate mean ± SD (n = 18). (**$p < 0.01$; *$p < 0.05$, Student's *t*-test).

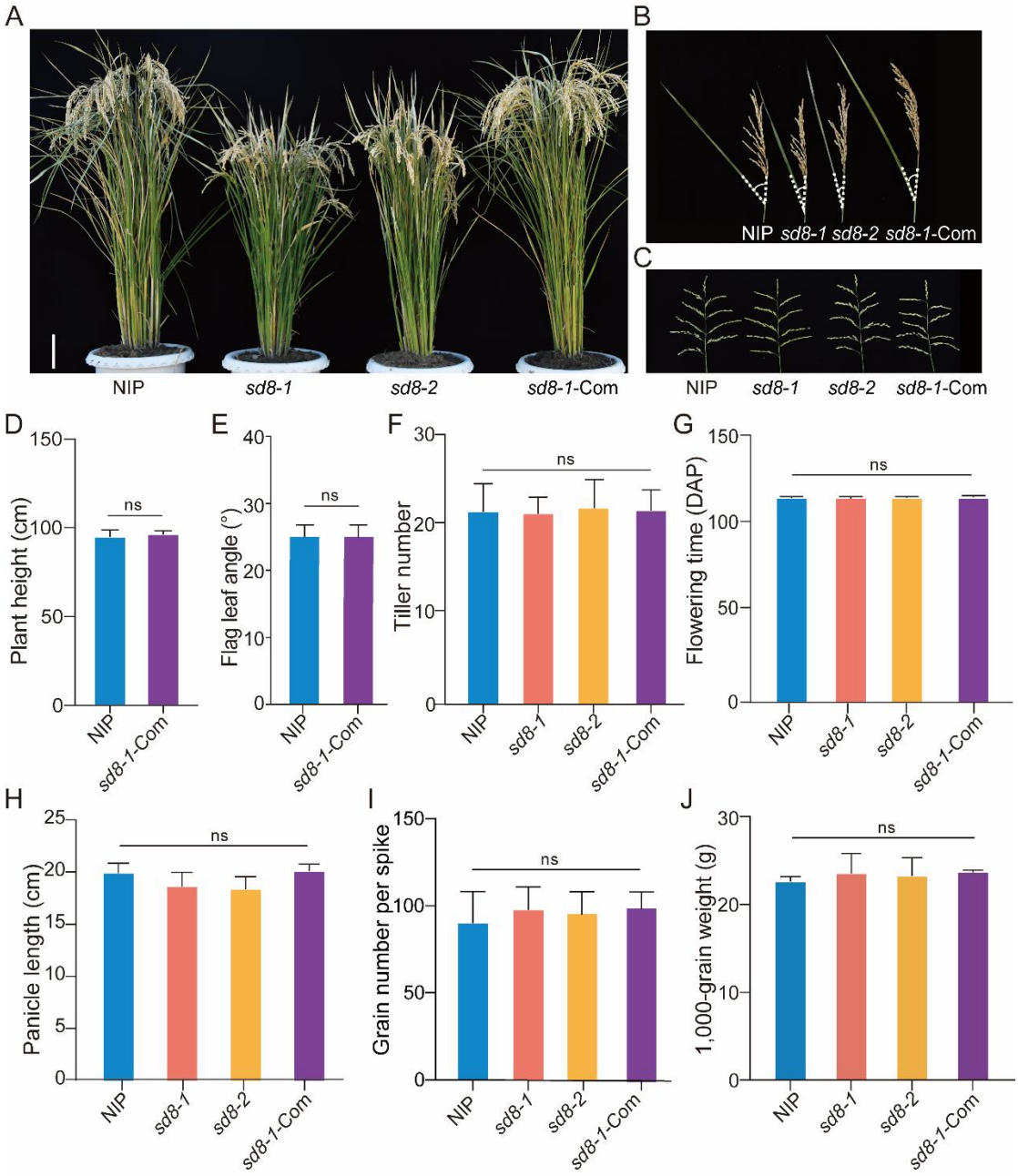

Supplementary Figure 2. Phenotypes of *SD8* KO and complemented lines.

(A) Plant architecture of mature stage NIP, *sd8-1*, *sd8-2,* and *sd8-1*-Com. (scale bar: 10 cm).

(B) The flag leaf angle in NIP, *sd8-1*, *sd8-2,* and *sd8-1*-Com plants.

(C) The panicle morphology in NIP, *sd8-1*, *sd8-2,* and *sd8-1*-Com plants.

(D) Comparison of plant height between NIP and *sd8-1*-Com.

(E) Comparison of flag angle between NIP and *sd8-1*-Com.

(F-J) Comparison of tiller number, flowering time, panicle length, grain number per spike, and 1,000-grain weight in NIP, *sd8-1*, *sd8-2,* and *sd8-1*-Com. Data represent

mean ± SD (n=24). (**$p < 0.01$; *$p < 0.05$, Student's *t*-test).

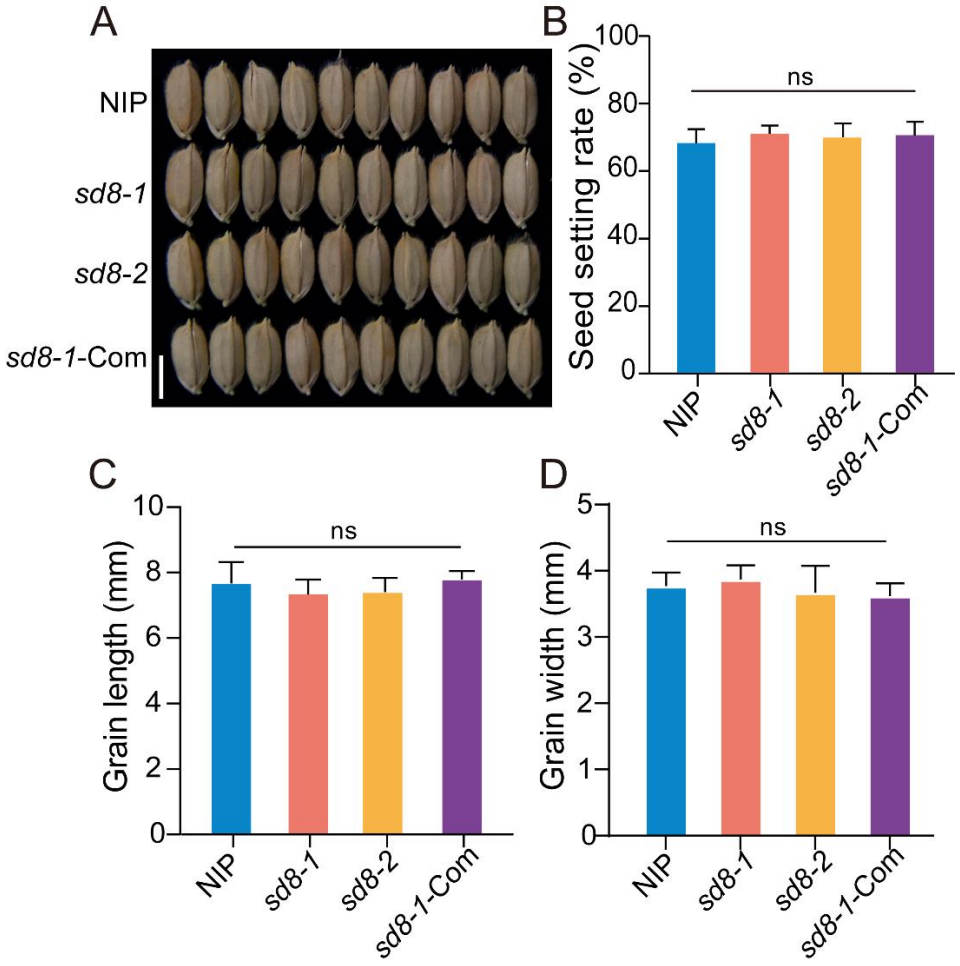

Supplementary Figure 3. *SD8* KO lines did not cause significant differences in grain morphology compared to NIP.

(A) Grain morphology of NIP, *sd8-1*, *sd8-2*, and *sd8-1*-Com. (Scale bar:0.5 cm).

(B) Comparison of seed setting rate in NIP, *sd8-1*, *sd8-2*, and *sd8-1*-Com. Data represent mean ± SD (n = 24).

(C-D) Statistical data of the grain length (C) and width (D). (**$p < 0.01$; *$p < 0.05$, Student's *t*-test).

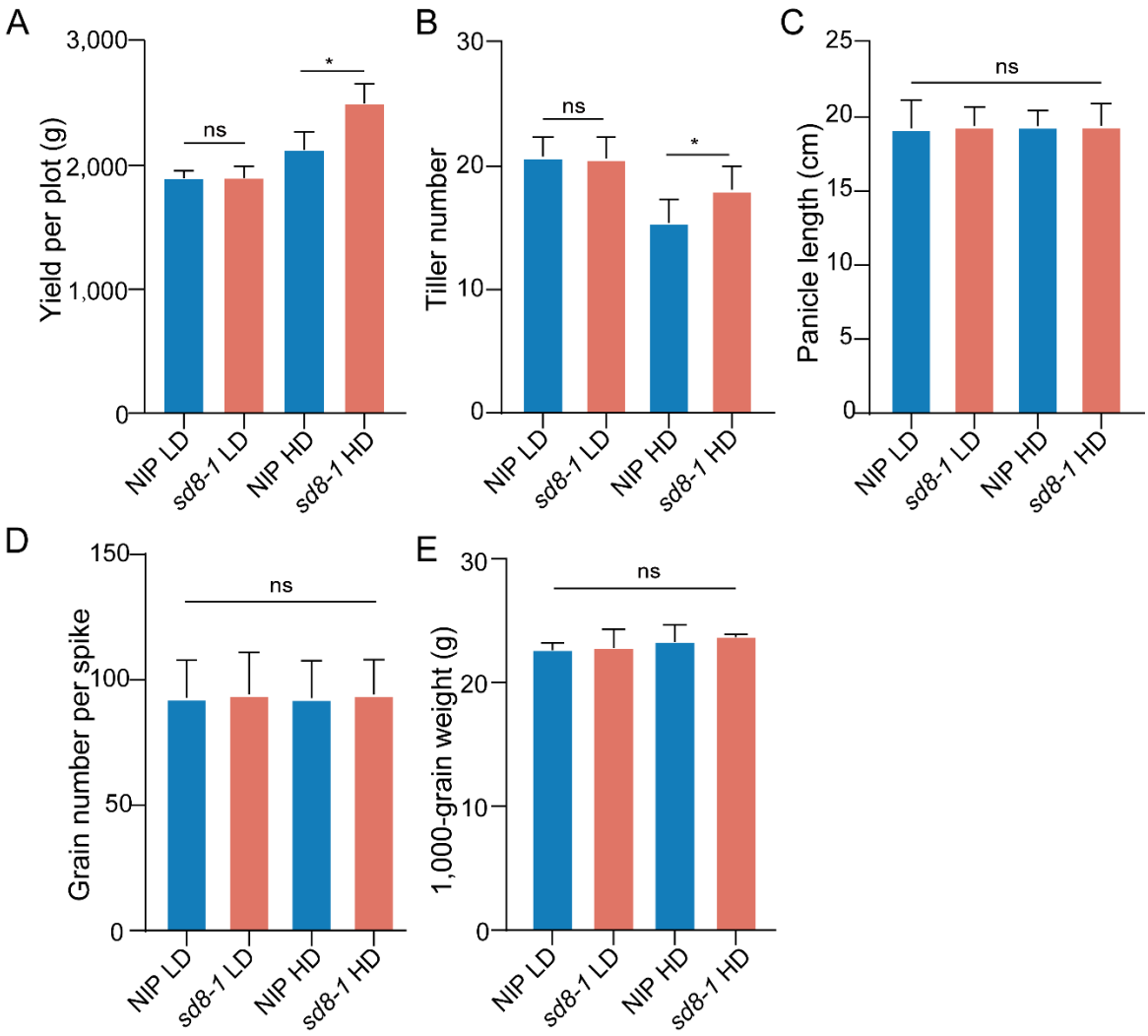

Supplementary Figure 4. Statistical data of grain yield per plot and yield-related traits in NIP and *sd8-1* under different planting density conditions.

(A) Grain yield per plot at high and low densities.

(B-E) Statistical data of yield-related traits in NIP and *sd8-1* under different planting density conditions. Different characters indicate significant differences. (**$p < 0.01$; *$p < 0.05$, Student's *t*-test).

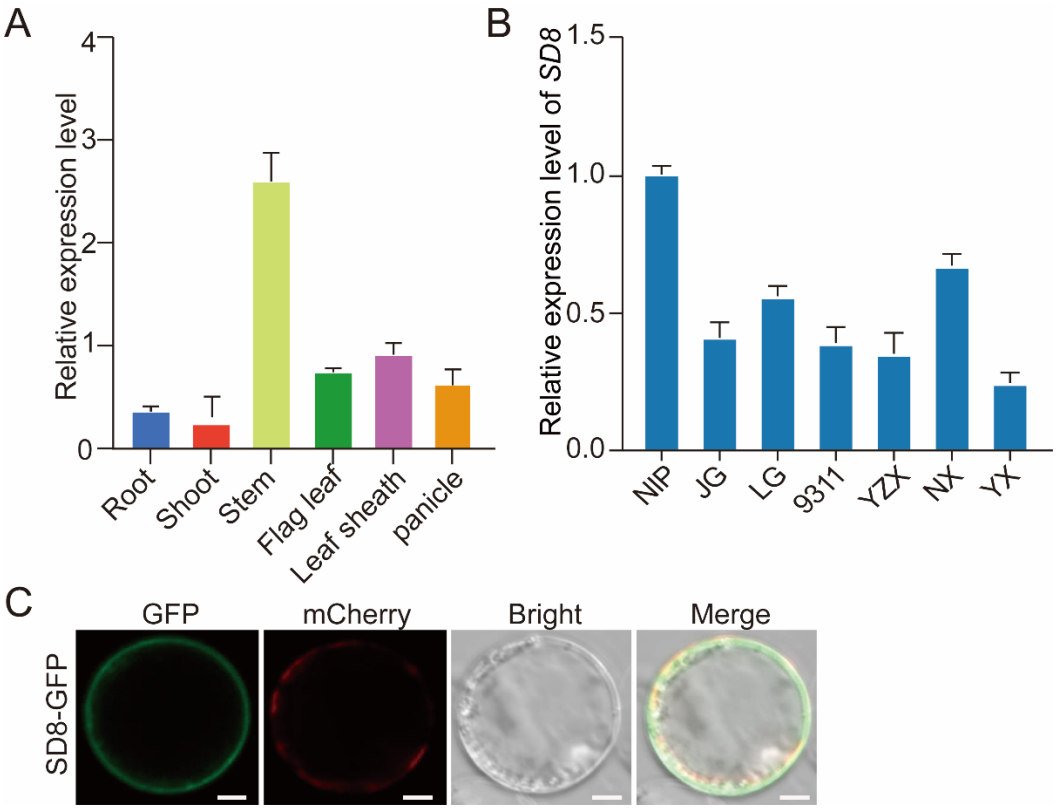

Supplementary Figure 5. Expression pattern of *SD8* and subcellular location of SD8.

(A) Relative expression level of *SD8* in each tissue of NIP at different growth stages. NIP was cultivated in normal culture solution for 3 weeks and transferred to the field. **(B)** Quantitative real-time PCR (qPCR) analysis of expression level of *SD8* between *indica* (9311, YZX, NX, YX) and *japonica* (NIP, JG, LG) rice varieties. All qRT-PCR experiments were analyzed using three independent biological repeats. **(C)** Subcellular localization of SD8/OsABCB1 in rice protoplasts. (Scale bars:10 μm).

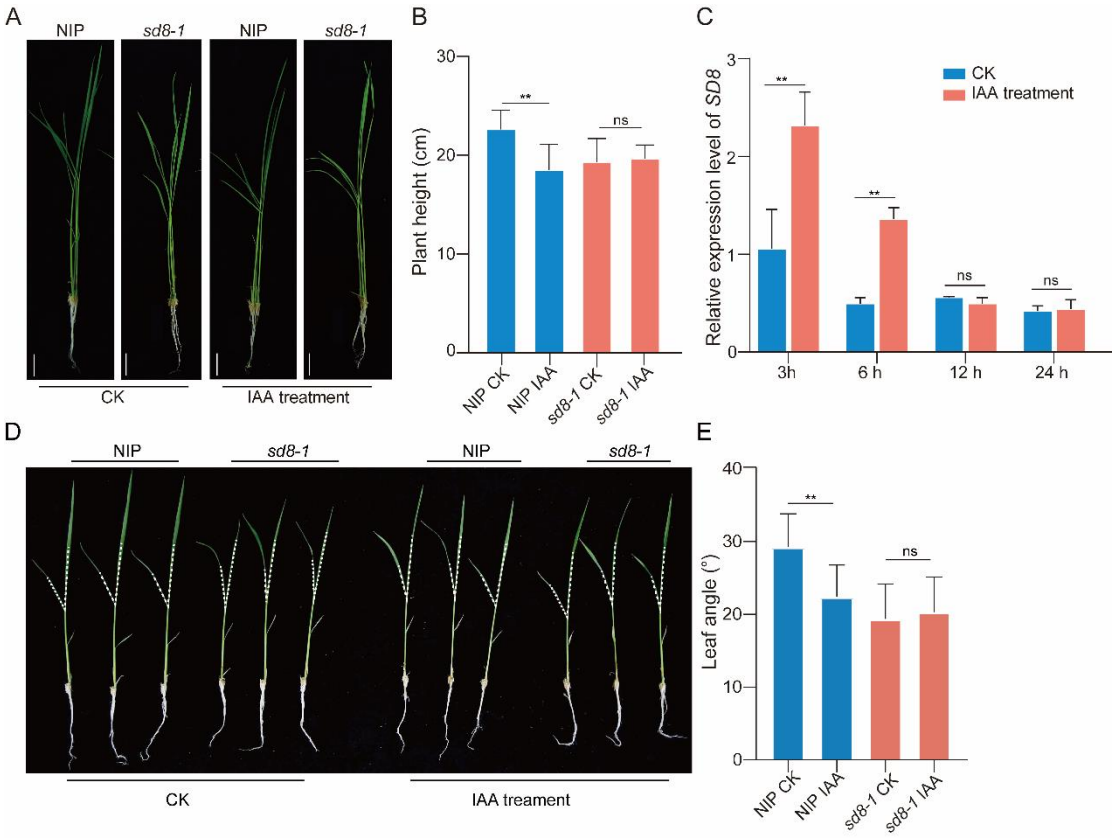

Supplementary Figure 6. Analysis of auxin response in NIP and *sd8-1*.

(A) Phenotype of NIP and *sd8-1* for 10-day-old seedlings under normal conditions (CK) and 10 μM IAA treatments 3 days. (Scale bars:2 cm).

(B) Statistical data of shoot length in NIP and *sd8-1* under 10 μM concentrations of IAA 3days.

(C) Expression of *SD8* in 10 μM IAA treatments at the indicated time intervals. 10-day-old seedlings grown in normal culture solution were exposed to 10 μM IAA treatments until shoots were sampled at the indicated time intervals. qRT-PCR experiments were analyzed using three independent biological repeats. The *OsACTIN* gene was used as an internal control.

(D) Phenotype of NIP and *sd8-1* for 7-day-old seedlings under normal conditions (CK) and 10 μM IAA treatments 4 days.

(E) Statistical data of leaf angle in NIP and *sd8-1* under 10 μM concentrations of IAA 4 days. Data represent mean ± SD (n=35). (**$p < 0.01$; *$p < 0.05$, Student's t-test).

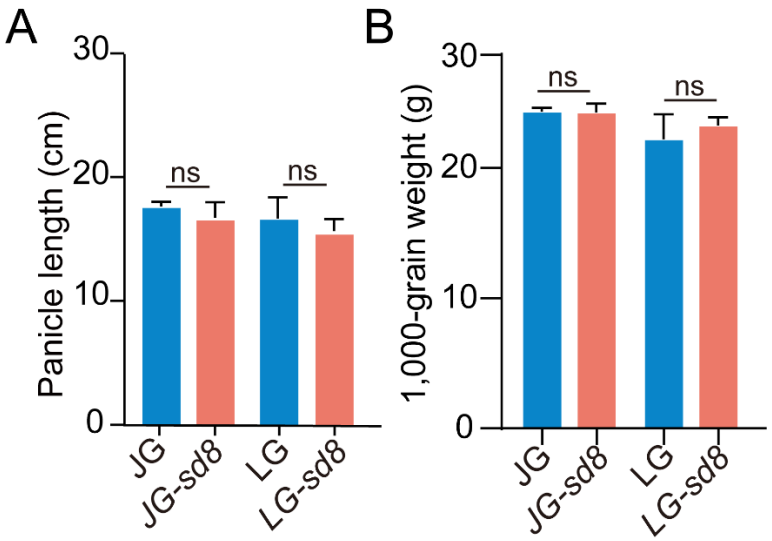

Supplementary Figure 7. Statistical data of plant height and 1,000-grain weight in wild type and *SD8* KO lines in the indicated backgrounds.

(A) Statistical data of plant height in wild type and *SD8* KO lines in JG and LG.

(B) Statistical data of 1,000-grain weight in wild type and *SD8* KO lines in JG and LG. (**$p < 0.01$; *$p < 0.05$, Student's *t*-test).

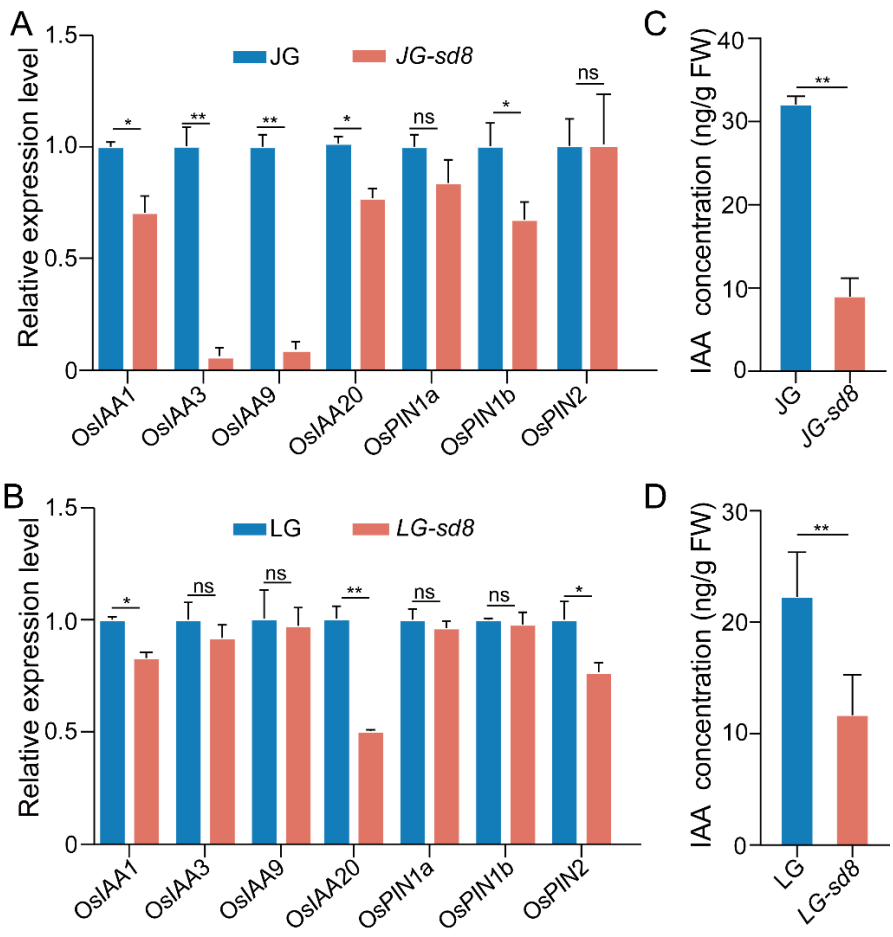

Supplementary Figure 8. qRT-PCR analysis for auxin-responsive genes and the relative content of free IAA in JG, *JG-sd8*, LG, and *LG-sd8* lines.

(A-B) Relative expression levels of *OsIAA1/3/9/20* and *OsPIN1a/1b/2* in 3-week-old seedlings of JG, *JG-sd8* (A), LG, and *LG-sd8* lines (B) *OsACTIN* gene was used as an internal control. All qRT-PCR experiments were analyzed using three independent biological repeats. (**$p < 0.01$; *$p < 0.05$, Student's *t*-test).

(C-D) The relative content of free IAA in 3-week-old seedlings of JG, *JG-sd8*(C), LG, and *LG-sd8* lines (D).

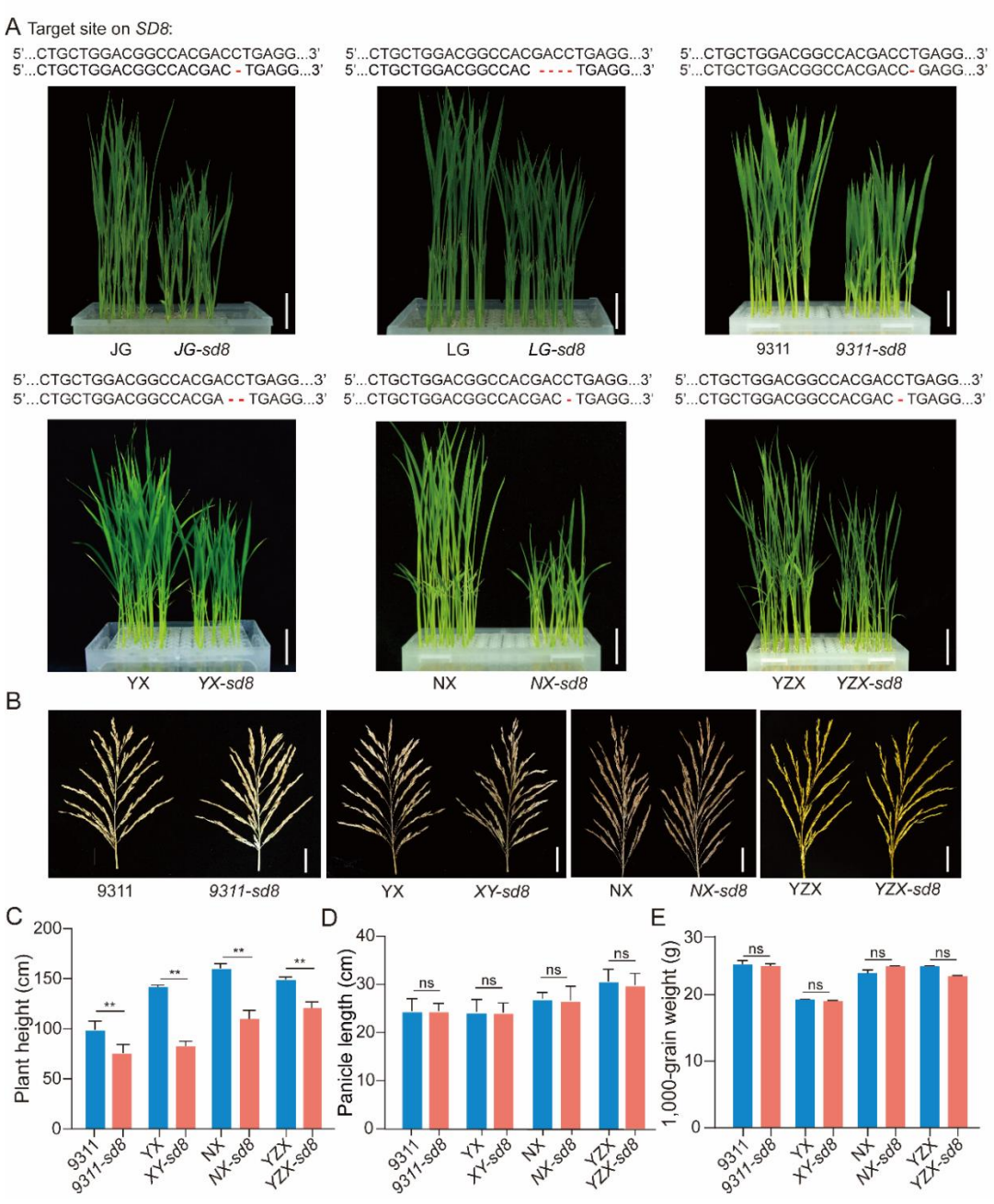

Supplementary Figure 9. *SD8* KO lines in *japonica* rice variety Jingeng818 (JG), Longgeng 31 (LG) and *indica* rice variety 93-11, YexiangB (YX), Nongxiang32 (NX), and Yuzhenxiang (YZX) backgrounds.

(A) Phenotypes of *SD8* KO lines in the indicated backgrounds. (Scale bars:2 cm).

(B) Panicle phenotype of wild type and *SD8* KO lines in NX, 9311, YX, and YZX backgrounds. (Scale bars:5 cm).

(C) Statistical data of plant height in wild type and *SD8* KO lines in 9311, YX, YZX, and NX.

(D) Statistical data of panicle length in wild type and *SD8* KO lines in the indicated backgrounds.

(E) Statistical data of 1,000-grain weight in wild type and *SD8* KO lines in the indicated backgrounds. (**$p < 0.01$; *$p < 0.05$, Student's *t*-test).

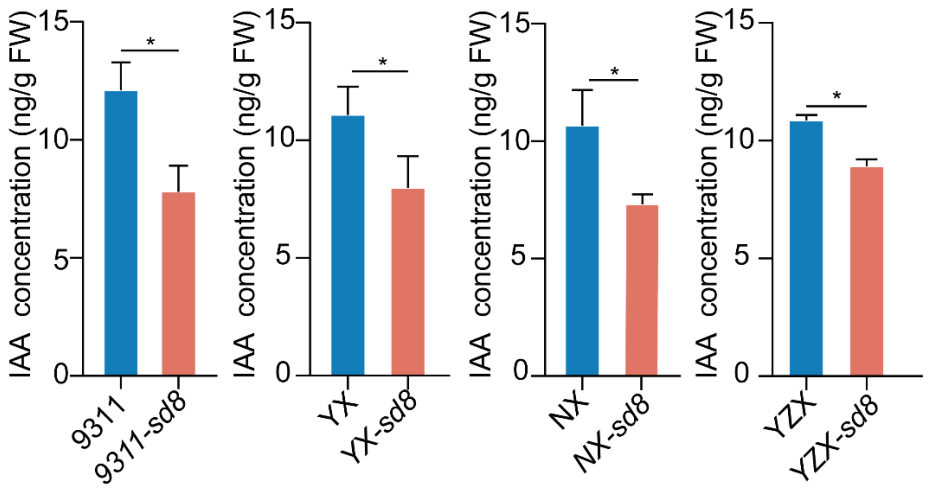

Supplementary Figure 10. The relative content of free IAA in wild type and *SD8* KO lines in the indicated backgrounds. GC-MS analysis of endogenous free IAA concentrations in wild type and *SD8* KO lines in the indicated backgrounds. All experiments were analyzed using three independent biological repeats. (**$p < 0.01$; *$p < 0.05$, Student's *t*-test).

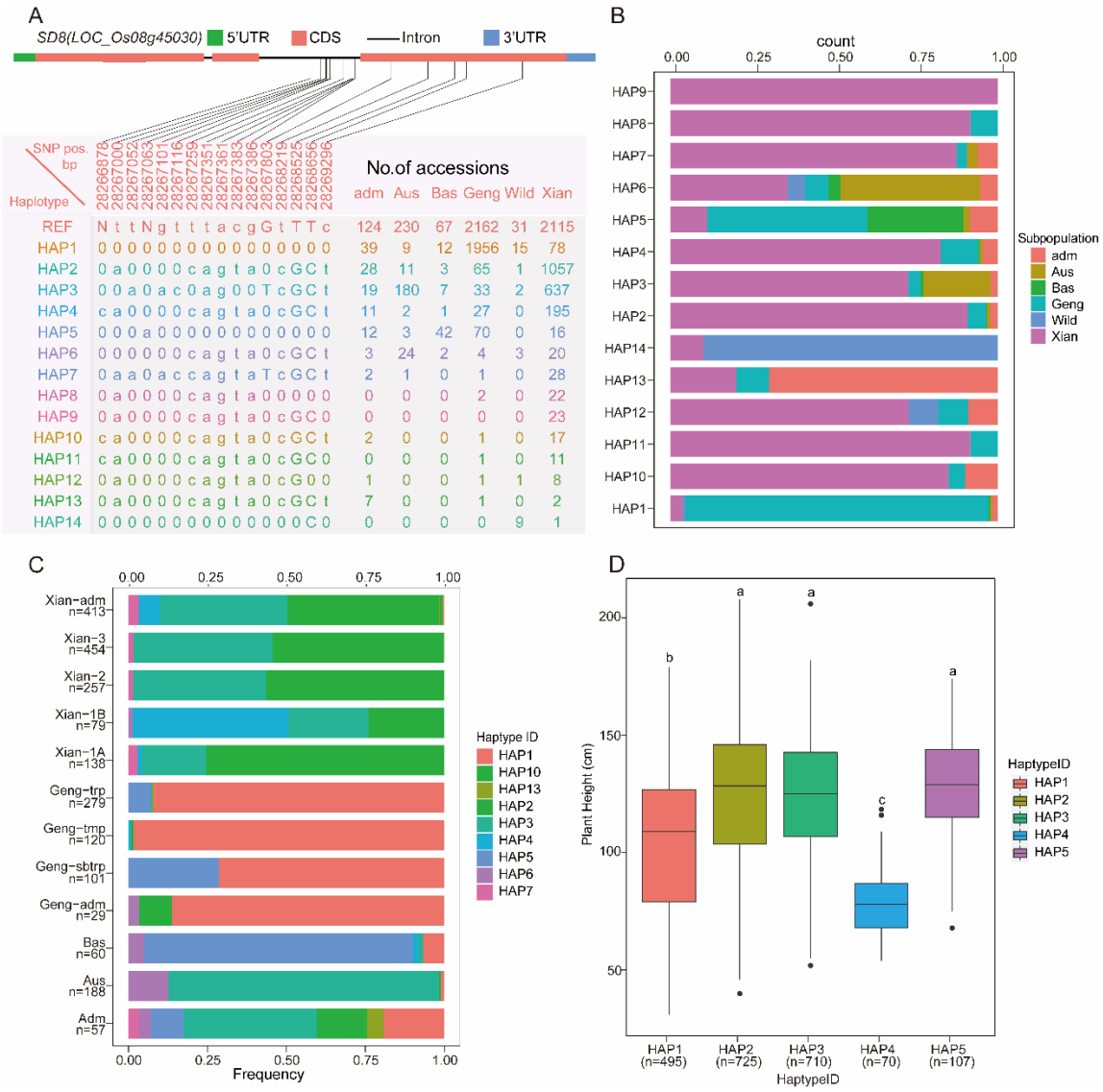

Supplementary Figure 11. Genetic diversity of *SD8* in the 3K RG dataset.

(A) Haplotypes of *SD8* (*LOC_Os08g45030*) in 1,978 accessions of 3K RG (rare haplotypes of <100 accessions are not shown) using 5 SNPs in the CDS region. Lowercase letters represent synonymous mutations, whereas uppercase letters indicate non-synonymous mutations.

(B) Haplotype network of *SD8* in 3K RG.

(C) Haplotype frequency of *SD8* in subpopulations of 3K RG.

(D) Performance distribution of different haplotypes of *SD8* in 3K RG. Different letters on plant height in 3K RG. Different letters on the boxplots indicate statistically significant differences (n = Hap number; p<0.01, Duncan's new multiple range tests).

292 **Table S1.** The primers for qRT-PCR analysis of *SD8*, *OsIAAs*, *OsPINs*.

Gene name	Forward primer 5'-3'	Reverse primer 5'-3'
SD8	CTGTCCAGCACCTCTTCTGG	GTCCTCCATGTCGAACCAGG
OsIAA1	GCCGCTCAATGAGGCATT	GCTTCCACTTTCTTTCAATCCAA
OsIAA3	AACTGAACAACAACAAGAAGAA	GCAATGAGGAGATGAGATGA
OsIAA9	AAGAAAATGGCCAATGATGATCA	CCCATCACCATCCTCGTAGGT
OsIAA9	TTGTACGTGAACGGGATTATTTTG	CATGCTTATGAAATTGCTGAAACA
OsPIN1a	TCATCTGGTCGCTCGTCTGC	CGAACGTCGCCACCTTGTTC
OsPIN1b	TGCACCCTAGCATTCTCAGCA	CCCTCCTCCCAAATTCTACTTC
OsPIN2	CAGGGCTAGGAATGGCTATGT	GCAAACACAAACGGGACAA

293

294

SI References

Geng, Y., Zhang, P., Liu, Q.,Wei, Z., Riaz, A., Chachar, S., and Gu, X. (2020). Rice homolog of Sin3-associated polypeptide 30, OsSFL1, mediates histone deacetylation to regulate flowering time during short days. Plant Biotechnol. J. **18**:325-327.

Zhang, P., Zhu, C., Geng, Y., Wang, Y., Yang, Y., Liu, Q., Guo, W., Chachar, S., Riaz, A., Yan, S., et al. (2021). Rice and *Arabidopsis* homologs of yeast CHROMOSOME TRANSMISSION FIDELITY PROTEIN 4 commonly interact with Polycomb complexes but exert divergent regulatory functions. Plant Cell **33**:1417-1429.

Henrichs, S., Wang, B., Fukao, Y., Zhu, J., Charrier, L., Bailly, A., Oehring, S.C., Linnert, M., Weiwad, M., Endler, A., et al. (2012). Regulation of ABCB1/PGP1-catalysed auxin transport by linker phosphorylation. EMBO J. **31**:2965-2980.

Alexandrov, N., Tai, S., Wang, W., Mansueto, L., Palis, K., Fuentes, RR., Ulat, VJ., Chebotarov, D., Zhang, G., Li, Z., et al. (2015). SNP-Seek database of SNPs derived from 3000 rice genomes. Nucleic Acids Res. **43**:1023-1027.

Vilella, A., Blanco-Garcia, A.,Hutter, S., Rozas, J. (2005). Analysis of evolutionary patterns from large-scale DNA sequence polymorphism data. Bioinformatics. **21**:2791–2793.

Yang, T., Feng, H., Zhang, S., Xiao, H., Xu, G. (2020). Potassium transporter OsHAK5 alters rice architecture via ATP-dependent transmembrane auxin fluxes. Plant Com. **1**:100052.

Prusty, R., Grisafi, P., Fink, G.R. (2004). The plant hormone indoleacetic acid induces invasive growth in Saccharomyces cerevisiae. Proc. Natl. Acad. Sci. U S A. **101**:4153–4157.

Yang, T., Zhang, S., Hu, Y., Wu, F., Hu, Q., Chen, G., Cai, J., Wu, T., Moran, N., Yu, L., et al. (2014). The role of a potassium transporter OsHAK5 in potassium acquisition and transport from roots to shoots in rice at low potassium supply

levels. Plant Physiol. **166**:945–957.

Wang, W., Mauleon, R., Hu, Z., Chebotarov, D., Tai, S., Wu, Z., Li, M., Zheng, T., Fuentes, RR., Zhang, F., et al. (2018). Genomic variation in 3,010 diverse accessions of Asian cultivated rice. Nature **557**:43-49.

Bradbury, PJ., Zhang, Z., Kroon, D.E., Casstevens, T.M., Ramdoss, Y., Buckler, E. S. (2007). TASSEL: software for association mapping of complex traits in diverse samples. Bioinformatics. **23**:2633.

Duan, P., Xu, J., Zeng, D., Zhang, B., Geng, M., Zhang, G., Huang, K., Huang, L., Xu, R., Ge, S., et al. (2017). Natural variation in the promoter of GSE5 contributes to grain size diversity in rice. Mol. Plant **10**:685-694.